



## Characterization of Corrosion Layer of Carbon Steel by Micro-PIXE/RBS Analysis

著者	Matsuyama S., Ishii K., Fujiwara M., Kikuchi Y., Nakhostin M., Kawamura Y., Tsuboi S., Yamanaka K., Watanabe M., Ohkura S., Hashimoto Y., Fujikawa M., Catella G., Fujiki K., Hatori Y., Hamada N., Tanino S., Abe H., Watanabe Y., Yamazaki H.
journal or publication title	CYRIC annual report
volume	2009
page range	99-103
year	2009
URL	<a href="http://hdl.handle.net/10097/50495">http://hdl.handle.net/10097/50495</a>

## V. 5. Characterization of Corrosion Layer of Carbon Steel by Micro-PIXE/RBS Analysis

*Matsuyama S.<sup>1</sup>, Ishii K.<sup>1</sup>, Fujiwara M.<sup>1</sup>, Kikuchi Y.<sup>1</sup>, Nakhostin M.<sup>1</sup>, Kawamura Y.<sup>1</sup>, Tsuboi S.<sup>1</sup>, Yamanaka K.<sup>1</sup>, Watanabe M.<sup>1</sup>, Ohkura S.<sup>1</sup>, Hashimoto Y.<sup>1</sup>, Fujikawa M.<sup>1</sup>, Catella G.<sup>1</sup>, Fujiki K.<sup>1</sup>, Hatori Y.<sup>1</sup>, Hamada N.<sup>1</sup>, Tanino S.<sup>1</sup>, Abe H.<sup>1</sup>, Watanabe Y.<sup>1</sup>, and Yamazaki H.<sup>2</sup>*

<sup>1</sup>*Department of Quantum Science and Energy Engineering, Tohoku University*

<sup>2</sup>*Cyclotron and Radioisotope Center, Tohoku University*

### Introduction

Piping, vessels and components of nuclear and thermal power plants are made of carbon steel or stainless steel. During plant operation, the protective oxide layer (magnetite or hematite) is formed on the surface of carbon steel where exposed to high temperature water flow and vapor. Wall thinning of piping made of carbon steel results from dissolution of the oxide layer. This phenomenon is a common problem in all types of these power plants and affects their lifetime and safety. Many factors such as flow rate, temperature, pH, dissolved oxygen concentration and composition of carbon steel affect corrosion rate. Especially water flow rate strongly affects the corrosion rate. This phenomenon is known as flow-accelerated corrosion (FAC)<sup>1)</sup>. FAC rate depends on many parameters such as water chemistry, temperature, mass transfer coefficient and chromium content in steel. Especially, chromium content is known as an important parameter to reduce the FAC rate. Chromium content higher than 0.05 wt% greatly reduces FAC rate. However, the chromium content is not regulated in carbon steel, or chromium is considered as mere impurity, so far. While the mechanism of this phenomena is not known perfectly yet, the chromium content seems to affect formation and dissolution on the oxide layer. Considering welded part of carbon steel, for examples, in which the segregation of chromium carbide are occurred along grain boundary, the reduction of thickness due to the process of oxide formation and dissolution takes place in the localized area around grain boundary. Therefore, oxide formation and dissolution should be related to the mechanism of corrosion. In order to understand the mechanism of the phenomenon of corrosion, characterization of oxide layer in the localized area is indispensable from this point of view.

For surface analysis of the oxide layer, many techniques such as secondary electron microscopy, X-ray diffraction, and transmission electron microscopy are used. However, complete elemental information, which is important for characterization, is not obtained by these methods. In this study, the simultaneous micro-PIXE/RBS analysis was applied to obtaining elemental characterization on oxide layer formed on the carbon steel.

### **Analysis system**

Analyses of samples were carried out with the microbeam system at Tohoku University. Technical details of the system were presented in previous papers<sup>2,3</sup>. Simultaneous PIXE/RBS analysis was conducted with the proton beam energy of 2.4 MeV and 3 MeV, the beam spot size of  $1 \times 1 \mu\text{m}^2$  and beam currents of around 50 pA. The beam scanning area was set to  $20 \times 20 \mu\text{m}^2$ . The quantitative PIXE analysis was performed using the GeoPIXEII software<sup>5</sup>. Light elements (C,N,O) were quantified by analyzing the extracted RBS spectra using the SIMNRA software<sup>6</sup>.

### **Results of analyses**

Samples are plates of carbon steel (1mm thick) with various chromium contents ranging from 0.003 wt% to 1.01 wt% (nominal). These samples were oxidized in water with and without flow in an autoclave. In dynamic oxidation condition, the water was conditioned at pH=9.07 and 9.36 by addition of ammonia under a flow rate of 3 m/sec. Under static condition, the water was conditioned at pH=7.

In the RBS analysis, two layers which correspond to oxide layer and base metal were considered. The corresponding cross sections for carbon, nitrogen, and oxygen were derived from the refs. 7 and 8. Rutherford cross section was used for iron. Figure 1 shows number of atoms in the oxide layer as a function of chromium contents. Nominal chromium and iron ratios are consistent with those obtained by PIXE. Number of atoms in the oxide layer decrease with the increase of chromium content. Thickness of oxide layer is estimated to be  $0.3 \mu\text{m}$  for chromium content of 1.01 wt%. The atomic ratios of O:Fe were around 1:5 and 1.2:1, in the chromium content of 0.003-0.1 wt% and 0.4-1.01 wt%, respectively. In chromium content higher than 0.4 %, the atomic ratio of O:Fe is close to that of  $\text{Fe}_3\text{O}_4$ . The layer formed on the surface is mainly composed of magnetite. Number of oxygen of the oxide layer is lower than that of magnetite for chromium content lower than 0.1 wt%.

X-ray yield maps of chromium and iron are shown in Fig. 2 for carbon steel oxidized with water flow of 3 m/sec. X-ray yields are not uniform over the scanning area, which is related to the changes in the thickness of oxide layer. As well as self-absorption of X-rays in the layer, X-ray production cross section changes corresponding to energy-loss in the oxide layer X-ray yield decreases around 10% correspond to the increase of the magnetite layer of 1  $\mu\text{m}$ . X-ray intensities of iron and chromium vary from 50-100%, which means that thick oxide layer was formed nonuniformly on the surface. In contrast, oxide layer was formed uniformly in the non flow case as mentioned previously. When oxide layer thickness is not uniform over the region, analysis of RBS spectra is impossible. Position dependent oxide layer composition and thickness can be obtained by fitting the RBS spectra derived from each pixel. Considering low counting statistics for each pixel, spectrum fitting is impossible. Thus, we select the region where X-ray yield of iron is similar and obtained RBS spectra from the selected region. Typical RBS spectra are also shown in Fig. 2 together with the simulated result by the SIMNRA for the selected regions. The RBS spectra changes drastically correspond to oxide layer thickness and compositions. In the simulation, three oxide layers have to be considered to fit the spectra. Oxide concentration is highest in the surface layer. Round shape of the edges corresponds to the decrease of oxide concentration toward the inside. While oxygen concentration is the same in the regions 1 and 2, carbon concentration in the region 1 is more than 2 times higher than that in the region 2. Since segregation of chromium carbide occurred along grain boundary, it will be suggested that the region 1 will be the oxide layer along the grain boundary. From the PIXE analysis, chromium and iron ratio is constant in these regions and same as the nominal value. Since PIXE analyze the elements in the ca. 10  $\mu\text{m}$  from the surface when the substrate assumes to be iron for 2.4 MeV protons, it may be difficult to find changes in chromium concentration in the thin layer.

On the other hand, the RBS spectra for chromium content of 1.01 wt% is quite different from the others. In region 1, number of protons scattered from oxygen and iron is quite low, compared to those in region 2 and carbon content is highest. In this simulation, 3 layers are considered and hydrogen must be introduced to fit the spectra. In both regions, hydrous metal oxide layer might be formed. Chromium and iron ratio is more than two times higher than the nominal value. Since layer thickness is thicker than the other case, chromium is concentrated in the layer. In region 1, chromium and iron ratio is 10% higher than that of region 2. It is apparent that chromium carbide is formed in the region 1.

## Conclusions

In order to know the mechanism of corrosion in the localized area, we applied the simultaneous micro-PIXE/RBS analysis to characterization of oxide layer. The simultaneous micro-PIXE/RBS system demonstrated the relation between chromium content and numbers of atoms of oxygen and of iron in the oxide layer for carbon steel oxidized under the static condition. The oxide layer formed at dynamic condition is not uniform even in the narrow area of  $20 \times 20 \mu\text{m}^2$ . In this case, it is difficult to characterize oxide layer by conventional RBS analysis. The simultaneous micro-PIXE/RBS system could characterize the layer by region analysis. By micro-PIXE analysis, a specific area was extracted as a region of interest to be analyzed by RBS. Then an RBS spectrum was extracted and analyzed by using the SIMNRA software so as to obtain the elemental composition of oxide layer. Under the dynamic condition, elemental composition of the oxide layer was strongly affected by chromium content. In the chromium content of 1.01 wt%, hydrous metal oxide layer was formed. Since chromium is concentrated in this layer, chromium carbide is formed and might be related to hydrous metal oxide. These results of this experiment obviously show the simultaneous micro-PIXE/RBS analysis system to be useful for better understanding of the corrosion mechanism.

## Acknowledgements

The authors would like to acknowledge the assistance of Fujisawa M. for maintenance and operation of the Dynamitron accelerator. The authors would like to thank Mr. Nagaya T. and Komatsu K., for their assistance in constructing the microbeam and target system.

## References

- 1) Sanchez-Caldera J. E., Griffith P., Rabinowicz E., Trans of the ASME, Engi, for Gas Turbines and Power, **110** (1988) 180.
- 2) Matsuyama S., Ishii K., Yamazaki H., Barbotteau Y., Amartivan Ts., Izukawa D., Hotta Mizuma K., Abe S., Oishi Y., Rodriguez M., Suzuki A., Sakamoto R., Fujisawa M., Kamiya T., Oikawa M., Arakawa K., Imaseki H., and Matsumoto N., *Int. J. PIXE*, **14** (2004) 1.
- 3) Matsuyama S., Ishii K., Abe S., Ohtsu H., Yamazaki H., Kikuchi Y., Amartaivan Ts., Inomata K., Watanabe Y., Ishizaki A., Barbotteau Y., Suzuki A., Yamaguchi T., Momose G., and Imaseki H., *Int. J. PIXE*, **15** (2005) 41.
- 4) Matsuyama S., Ishii K., Yamazaki H., Kikuchi Y., Inomata K., Watanabe Y., Ishizaki A., Oyama R., Kawamura Y., Yamaguchi T., Momose G., Nagakakura M., Takahashi M., and Kamiya T., *Nucl. Instr. and Meth.*, **B260** (2007) 55.
- 5) Ryan C. G., Van Achterbergh E., Yeats C. J., Driberg S. L., G. Mark, McInnes B. M., Win T. T., Cripps G. and Suter G. F., "Quantitative, high sensitivity, high resolution, nuclear microprobe imaging of fluids, melts and minerals", *Nucl. Instr. and Meth.*, **B188** (2002) 18.
- 6) Mayer M. SIMNRA Users's Guide, Technical Report IPP 9/113, MPI Plasmaphy.

- 7) Amirikas R., Jamieson D. N., and Dooley S. P., *Nucl. Instr. and Meth.*, **B77** (1993) 110.
- 8) Ramos A. R., Paul A., Rijniers L., F.da Silva M., and Soares J. C., *Nucl. Instr. and Meth.*, **B190** (2002) 95.

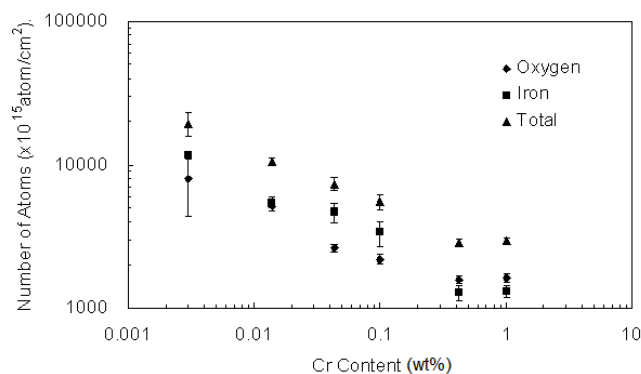


Figure 1. Number of atoms in the Oxide Layer as a Function of Chromium Content.

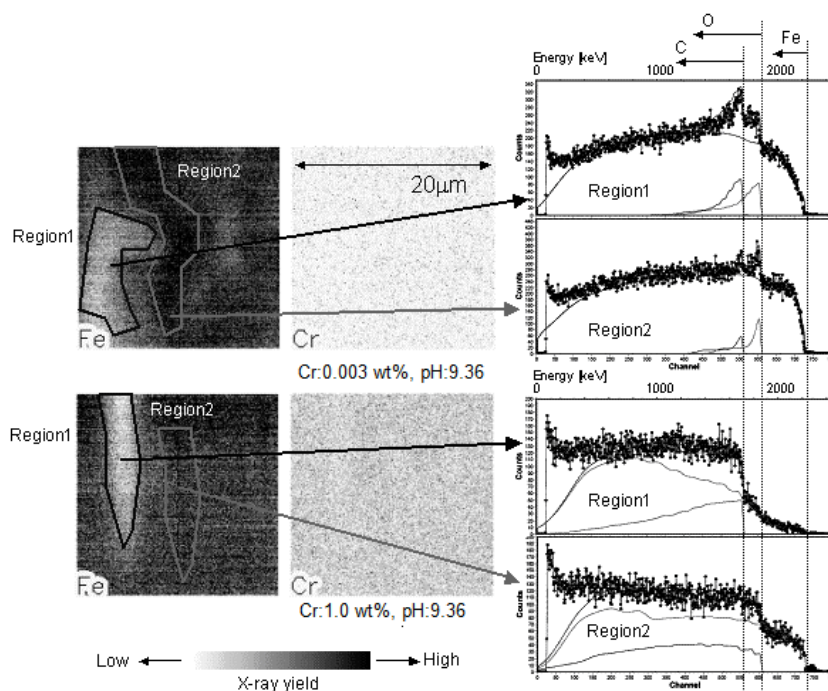


Figure 2. Typical Elemental Maps and RBS spectra of Chromium and Iron for Carbon Steel Oxidized under Dynamic Condition.

Upper : chromium content=0.003 wt% , pH = 9.37 and Lower: chromium content = 1.01 wt%, pH = 9.37